Group 50

Technical report
Energy Storage and Transport project

Eindhoven, September 7, 2025

Technische Universiteit Eindhoven University of Technology
TU/e

Group members (given name, surname, student ID):

Gábor, Bezsilla, 2155516

Job, van Driel, 2147696

Ice, Gerards, 2122545

Krzesimir, Hyżyk, 2084260

Arya, Katalmohseni, 2083574

Francesco Salvatore, 2118297

Date:	**Group number:**
September 7, 2025	Group 50

Coach/teacher:

Kayleigh K. Williams

Tutor:

Jarno van Tuil

Contents

1 Energy storage and transport system

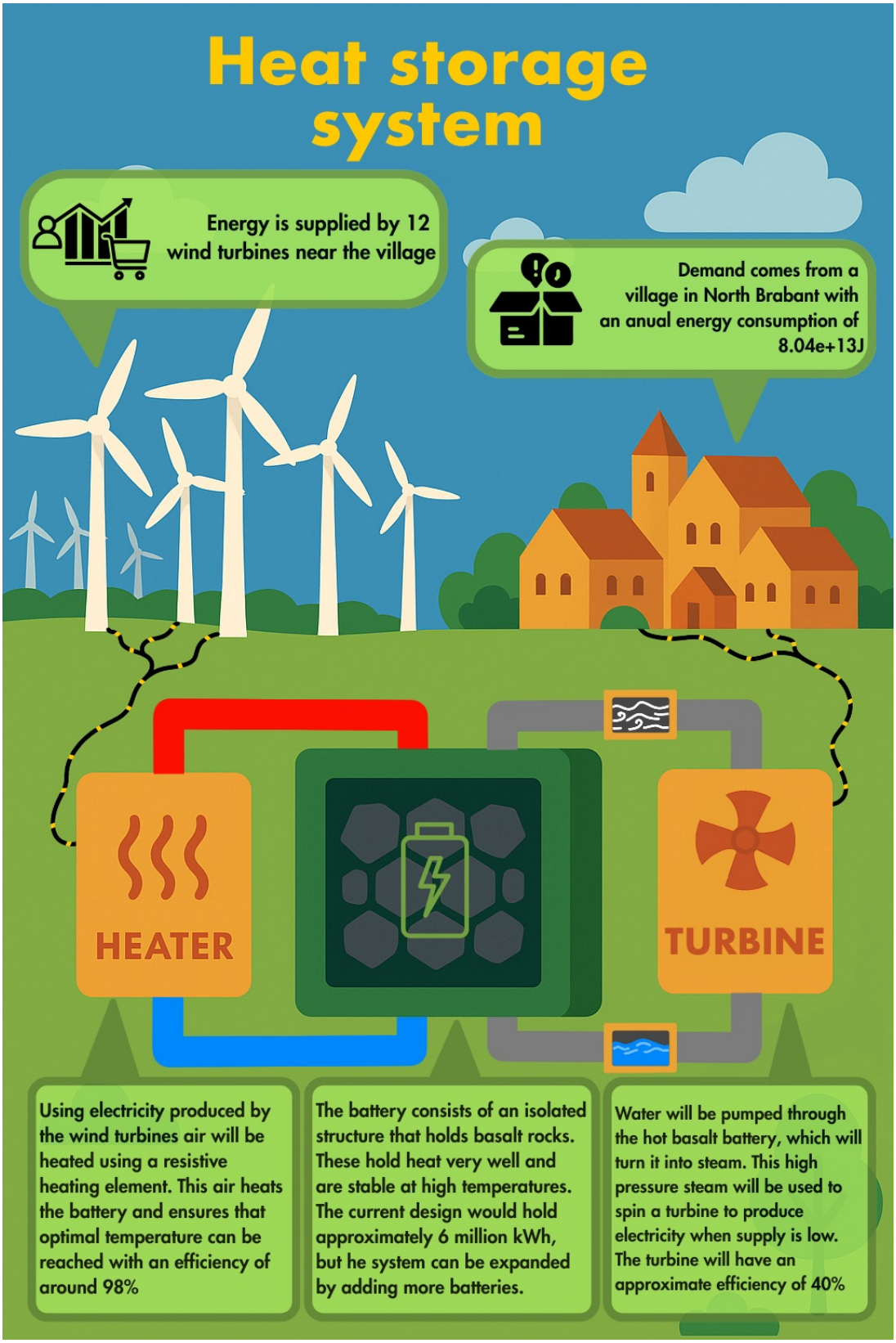

2 MATLAB/Simulink model implementation

2.1 The canvas (block structure)

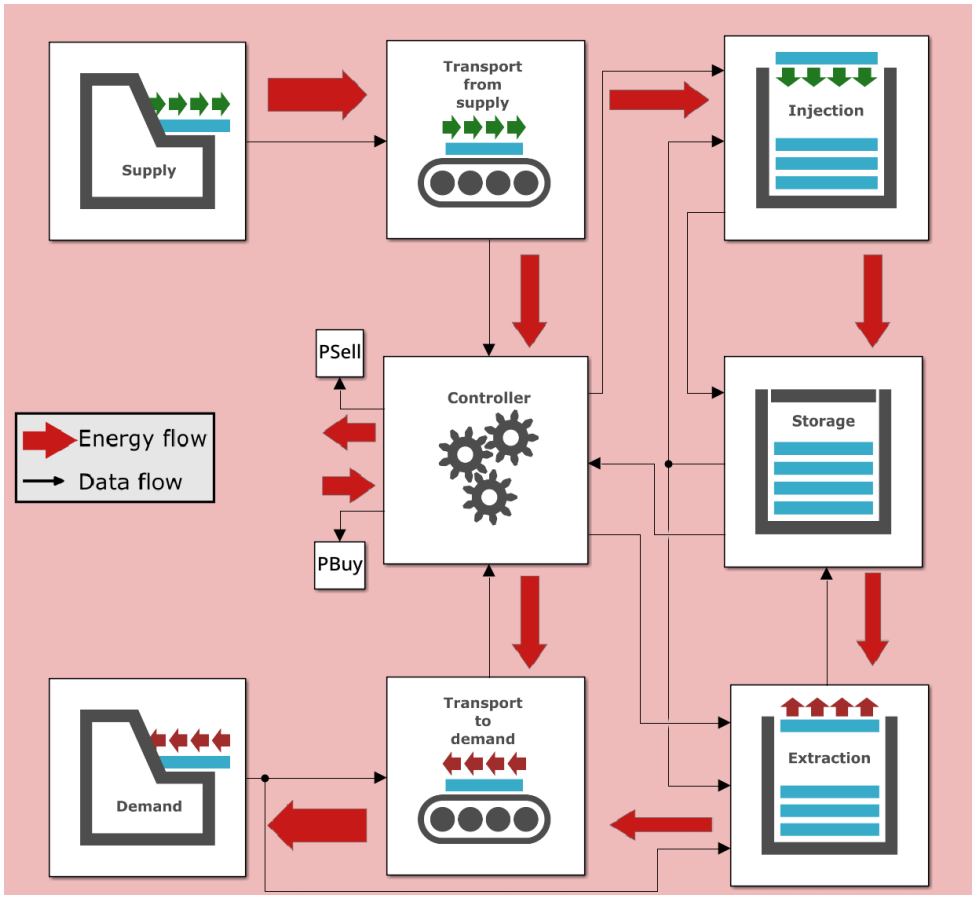

2.2 System parameters

```
const_simulation_variation_type="base";

const_environment_air_convection_heat_coefficient=5*unit("W/m^2/K");
const_environment_air_viscosity=1.715e-5*unit("Pa*s");
const_environment_pressure=101325*unit("Pa");
const_environment_specific_gas_constant=287.05*unit("J/kg/K");
const_environment_specific_heat_capacity_at_constant_pressure=12000*unit("Pa");
const_environment_stefan_boltzmann_constant=5.6704*unit("W/m^2/K^4");
const_environment_sutherland_constant=111*unit("K");
const_environment_temperature=293.15*unit("K");

const_transport_fan_heating_power=14.5*unit("kW");
const_transport_insulation_thickness=0.1*unit("m");
const_transport_pipe_air_convection_heat_coefficient=100*unit("W/m^2/K");
const_transport_pipe_inner_radius=0.4*unit("m");
const_transport_pipe_insulation_thermal_conductivity=401*unit("W/m/K");
const_transport_pipe_length=1.5*unit("km");
const_transport_pipe_outer_radius=0.5*unit("m");
const_transport_pipe_thermal_conductivity=401*unit("W/m/K");

const_injection_air_specific_heat_capacity=1005*unit("J/kg/K");
const_injection_extra_air_volume_factor=0.1*unit("1");
const_injection_fluid_thermal_conductivity=0.024*unit("W/m/K");
const_injection_fluid_velocity=10*unit("m/s");
const_injection_heater_efficiency=0.98*unit("1");
const_injection_shape_factor=10*unit("1");
const_injection_solid_thermal_conductivity=3.5*unit("W/m/K");

const_storage_insulation_conduction_coefficient=0.2*unit("W/m/K");
const_storage_insulation_emissivity=0.72*unit("1");
const_storage_insulation_thickness=1*unit("m");
const_storage_material_density=3011*unit("kg/m^3");
const_storage_material_grain_size=0.05*unit("m");
const_storage_material_porosity=0.367*unit("1");
const_storage_material_specific_heat_capacity=900*unit("J/kg/K");
const_storage_max_temperature=1273.15*unit("K");

const_extraction_boiler_pressure=25*unit("MPa");
const_extraction_condenser_pressure=10*unit("kPa");
const_extraction_pipe_length=10*unit("m");
const_extraction_pipe_radius=0.1*unit("m");
const_extraction_pipe_thickness=0.0125("m");
const_extraction_pipe_material_conductivity=22.5*unit("J/kg/K");


if const_simulation_variation_type=="base"
        height=25.35*unit("m");
        radius=12.68*unit("m");
        const_storage_insulation_area=2*pi*radius*(radius+height);
        const_storage_volume=pi*height*radius^2;
elseif const_simulation_variation_type=="geometry"
```

```
        % cube instead of cylinder
        side_length=23*unit("m");
        const_storage_insulation_area=6*side_length^2;
        const_storage_volume=side_length^3;
elseif const_simulation_variation_type=="volume"
        % halved volume
        height=12.68*unit("m");
        radius=12.68*unit("m");
        const_storage_insulation_area=2*pi*radius*(radius+height);
        const_storage_volume=pi*height*radius^2;
elseif const_simulation_variation_type=="pressure"
        % modified pressure
        height=25.35*unit("m");
        radius=12.68*unit("m");
        const_storage_insulation_area=2*pi*radius*(radius+height);
        const_storage_volume=pi*height*radius^2;
        const_extraction_boiler_pressure=35*unit("MPa");
        const_extraction_condenser_pressure=7.5*unit("kPa");
else
        error("Unknown design variation");
end
```

2.3 The code for the mathematical-physical models

The following sections describe the mathematical-physical background of the Simulink model. The following table provides an insight into the used constants:

Constant (Environment)	Symbol	Value
Air pressure	P_{air}	101325 Pa
Air viscosity	μ_{air}	1.715×10^{-5} Pa · s
Convection heat coefficient	h_{air}	5 $\frac{\text{W}}{\text{m}^2\cdot\text{K}}$
Environment temperature	T_{env}	293.15 K
Specific gas constant	R	287.05 $\frac{\text{J}}{\text{kg}\cdot\text{K}}$
Specific heat capacity at constant pressure	c_{p}	12 kPa
Stefan-Boltzmann constant	σ	5.6704 $\frac{\text{W}}{\text{m}^2\cdot\text{K}^4}$
Sutherland constant	μ_0	111 K
Constant (Transport)	**Symbol**	**Value**
Convection heat coefficient (within pipes)	h_{pipe}	100 $\frac{\text{W}}{\text{m}^2\cdot\text{K}}$
Heating fan power	P_{fan}	14.5 kW
Inner pipe radius	r_{inner}	0.4 m
Insulation thickness	$t_{\text{insulation,pipe}}$	0.1 m
Outer pipe radius	r_{outer}	0.5 m
Pipe length	l_{pipes}	1.5 km
Thermal conductivity (insulation)	$k_{\text{insulation,pipe}}$	0.2 $\frac{\text{W}}{\text{m}\cdot\text{K}}$
Thermal conductivity (pipe)	k_{pipe}	401 $\frac{\text{W}}{\text{m}\cdot\text{K}}$
Constant (Injection)	**Symbol**	**Value**
Extra air volume	ϵ	10%
Fluid thermal conductivity	k_f	0.024 $\frac{\text{W}}{\text{m}\cdot\text{K}}$
Fluid velocity	v_f	10 $\frac{\text{m}}{\text{s}}$
Heater efficiency	η_{heater}	98%
Particle shape factor	β	10
Solid thermal conductivity	k_s	3.5 $\frac{\text{W}}{\text{m}\cdot\text{K}}$
Specific heat capacity (air)	c_{air}	1005 $\frac{\text{J}}{\text{kg}\cdot\text{K}}$
Constant (Storage)	**Symbol**	**Value**
Insulation conduction coefficient	$k_{\text{insulation,battery}}$	0.2 $\frac{\text{W}}{\text{m}\cdot\text{K}}$
Insulation emissivity	ε	0.72
Insulation thickness	$t_{\text{insulation,battery}}$	1 m
Material density	ρ_{basalt}	3011 $\frac{\text{kg}}{\text{m}^3}$
Material grain size	d_{basalt}	0.05 m
Material porosity	ϕ	0.367
Material specific heat capacity	c_{basalt}	900 $\frac{\text{J}}{\text{kg}\cdot\text{K}}$
Max temperature	T_{max}	1273.15 K

The variation-specific constants can be seen listed in the table below:

Parameter	Base	Geometry	Volume	Pressure
Boiler pressure (p_{boiler})	25 MPa	25 MPa	25 MPa	35 MPa
Condenser pressure ($p_{\text{condenser}}$)	10 kPa	10 kPa	10 kPa	7.5 kPa
Storage surface area (A_{battery})	3030 m^2	3174 m^2	2020 m^2	3030 m^2
Storage volume (V_{battery})	12805 m^3	12167 m^3	6405 m^3	12805 m^3

2.3.1 Injection

Injection is performed by the means of a fan and a heating element acting on a closed air cycle through the porous storage tank. Due to the non-zero porosity of the storage material, the following dynamic relations must be used to accurately model convection within the system. **??**

$$\begin{aligned}(1-\phi)(\rho c)_s \frac{\partial T_s}{\partial t} &= (1-\phi)\nabla\cdot(k_s\nabla T_s) + (1-\phi)q_s''' + h(T_f - T_s)\\ \phi(\rho c_p)_f \frac{\partial T_f}{\partial t} + (\rho c_p)_f\,\mathbf{v}\cdot\nabla T_f &= \phi\nabla\cdot(k_f\nabla T_f) + \phi q_f''' + h(T_s - T_f)\\ q''' &= h\cdot(T_f - T_s)\end{aligned}$$

By rearranging and solving for q''', the following volumetric heat flux equation was obtained:

$$q''' = \left(\frac{6(1-\phi)}{d_p}\cdot\left(\frac{d_p}{\text{Nu}_{fs}\cdot k_f} + \frac{d_p}{\beta\cdot k_s}\right)^{-1}\right)\cdot(T_f - T_s)$$

The obtained relation for the volumetric heat flux was applied in an iterative manner to the air-battery cycle, allowing for accurate heat injection modeling. It was observed that the largest mode of heat loss within the air cycle was through the battery medium itself, making it possible to simplify the model's final implementation.

2.3.2 Storage

The storage block is responsible for monitoring the battery's temperature and elucidate any possible losses that may occur within the system. The three key methods of heat loss are conduction, convection, and radiation. The combined equation was concluded to be the following:

$$R_{\text{total}} = \underbrace{\frac{\ln r_{\text{outer}} - \ln r_{\text{inner}}}{2\pi k L}}_{R_{\text{cond}}} + \underbrace{\frac{1}{2\pi r_{\text{outer}} h L}}_{R_{\text{conv}}} + \underbrace{\frac{T_{\text{battery}} - T_{\text{outside}}}{\sigma\epsilon A\left(T_{\text{battery}}^4 - T_{\text{outside}}^4\right)}}_{R_{\text{rad}}}$$

Where the battery's temperature is calculated as follows:

$$T_{\text{battery}} = T_{\text{outside}} + \frac{E}{Mc}$$

By combining the equations above, the following relation for the battery's energy change over time was derived:

$$\dot{E}_{\text{storage}} = \Delta P - \frac{T_{\text{battery}} - T_{\text{outside}}}{R_{\text{total}}}$$

This formula was integrated within the storage to block to provide continuous feedback on the storage temperature, required for the injection block to work correctly.

2.3.3 Extraction

The discharge cycle in the model follows a supercritical Rankine cycle complemented by a low-temperature organic Rankine cycle to increase efficiency. A Rankine cycle is a thermodynamic cycle extracting mechanical work from a fluid moving between a heat source and a heat sink, converting thermal energy into electricity in the process. In the case of our Simulink model, water was chosen as the fluid within the theoretical cycle, as existing MATLAB libraries for steam tables only account for it.

A Rankine cycle is characterized by four stages: pressurization [1→2], heating [2→3], cooling [3→4], and condensing [4→1] as seen in the following illustration:

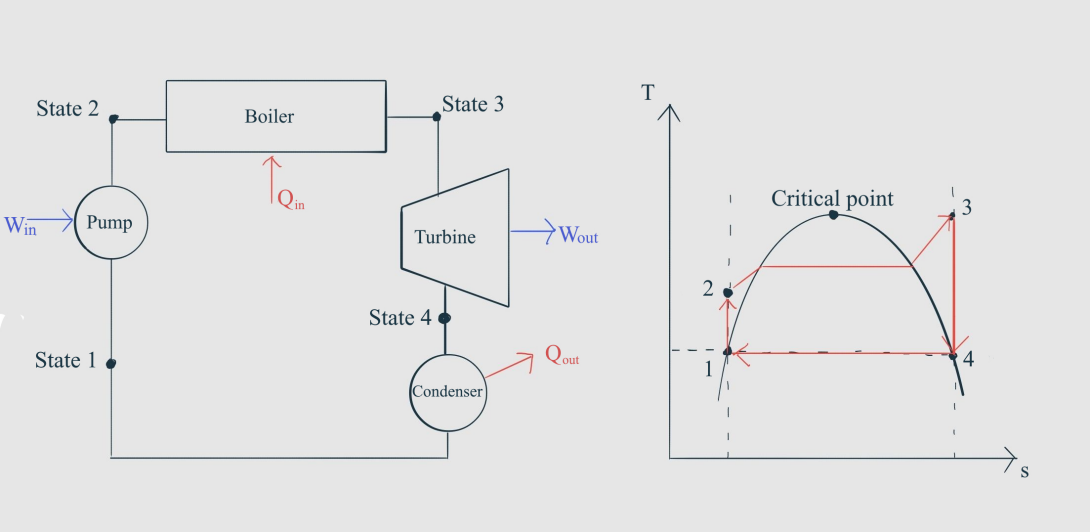

Figure 1: Ideal Rankine cycle

The physical foundation for the Rankine cycle is given by the following equations:

$$\frac{\dot{Q}_{\text{in}}}{\dot{m}} = h_3 - h_2 \qquad \frac{\dot{Q}_{\text{out}}}{\dot{m}} = h_4 - h_1 \qquad \frac{\dot{W}_{\text{pump}}}{\dot{m}} = h_2 - h_1 \qquad \frac{\dot{W}_{\text{turbine}}}{\dot{m}} = h_3 - h_4$$

Where the efficiency of a cycle is additionally given by the following relation:

$$\eta = \frac{\dot{W}_{\text{turbine}} - \dot{W}_{\text{pump}}}{\dot{Q}_{\text{in}}}$$

The computation of the cycle starts at state 1, the outlet of the condenser. As the condenser pressure is known, the specific volume, the enthalpy, and the temperature of the saturated liquid can all be determined from steam tables. In order to obtain these values, the XSteam MATLAB library was used within the project.

The enthalpy at state 2 is computed by adding the enthalpy at state 1 and the pump work, determined by the following expression:

```
% v1 (specific volume), h1, and T1 (T_fluid) are lookup up from
%pre-computed steam tables
wpump = v1 * (boiler_pressure - condenser_pressure) / 1e3; % kJ/kg
h2 = h1 + wpump; % kJ/kg
```

To calculate the enthalpy at state 3, the heat flow to the boiler must be determined. This heat flow is conducted through the piping of the heat exchanger inside the battery, therefore the formula for conduction within pipes is used:

$$\dot{Q} = 2\pi c r L \frac{T_{\text{battery}} - T_{\text{fluid}}}{t}$$

```
% Calculate h3 from h2 and h_in
h_in = Qin_dot / m_dot;
h3 = h2 + h_in / 1e3;  % kJ/kg
```

Lastly, the enthalpy at state 4 can be computed via steam tables (obtained from the XSteam library), making it possible to compute the overall efficiency of the cycle:

$$\eta = \frac{\dot{m}\left(\eta_{\text{generator}}\left(\frac{w_{\text{turbine}} - w_{\text{pump}}}{\dot{m}}\right) + \frac{Q_{\text{out}}}{\dot{m}}\eta_{\text{orc}}\right)}{\dot{Q}_{\text{in}}}$$

Where η_{orc} is the assumed efficiency of the low-temperature, organic Rankine cycle that is applied to the leftover heat. In the end, the total efficiency is substituted into the extraction function, yielding the following final extraction power calculation:

```
% Output efficiency needs to be inserted into the given form
DExtraction = output_eff / (1-output_eff) * PfromExtraction;
PtoExtraction = PfromExtraction + DExtraction;
```

3 Model application

3.1 The simulation scenario

The simulation scenario models a wind farm equipped with 12 turbines near a village in North Brabant, supplying Households in a nearby village with an annual energy consumption of 8.04×10^{13} J.

The challenge to overcome is to save the surplus of wind farm energy produced, and to distribute it so that it can be used throughout the year when there is a deficiency in the amount of energy production. After studying multiple forms of energy storage, it was concluded that given the supply and demand, heat energy storage would be ideal for this scenario, as it could store large amounts of energy provided by the farm for prolonged periods of time.

The simulation follows a concept of a thermal battery that utilizes basalt as the storage medium. The excess energy warms up the battery through an air cycle. The battery's heat is used to create supercritical steam that spins the turbines, which supply the town with electricity when demand outgrows supply, but the battery is charged.

3.2 Results and interpretation

The results of the simulation are presented through a series of figures that illustrate the performance of the heat energy storage (EST) system in managing the power generated by the wind farm. Figure 2 shows the supply given by the wind farm and the demand from the nearby village. As mentioned above, there are large spikes present in production with prolonged periods of minimal supply, which is precisely why the heat storage system was chosen.

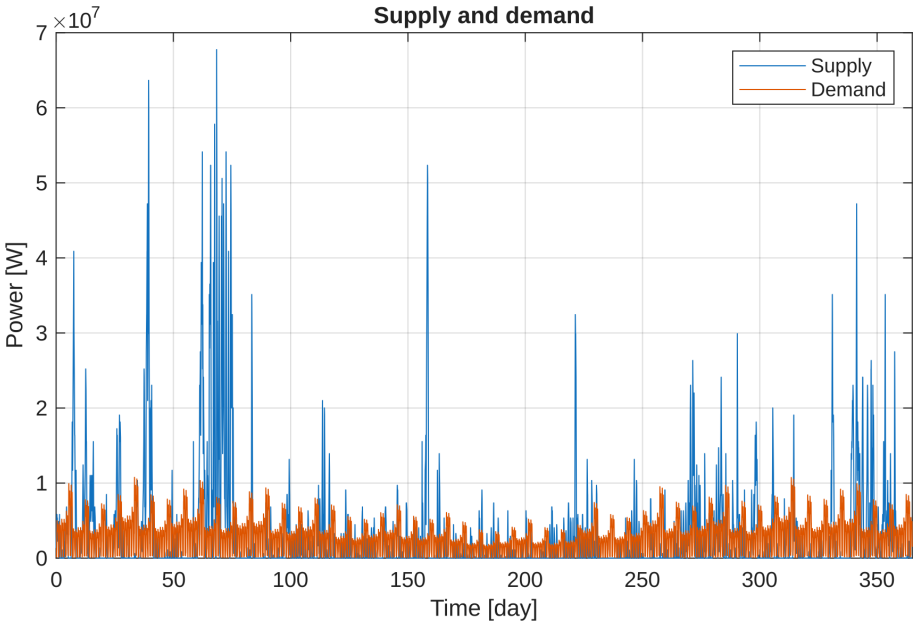

Figure 2: Supply and Demand

When measuring the energy stored inside the system, the most convenient way is to observe its internal temperature. Figure 3 illustrates the temperature profile within the thermal battery over the simulated year. More specifically, the temperature of the basalt within the system. This figure further shows that most of the energy is stored over the spikes within the supply, as the battery heats up the most during these periods.

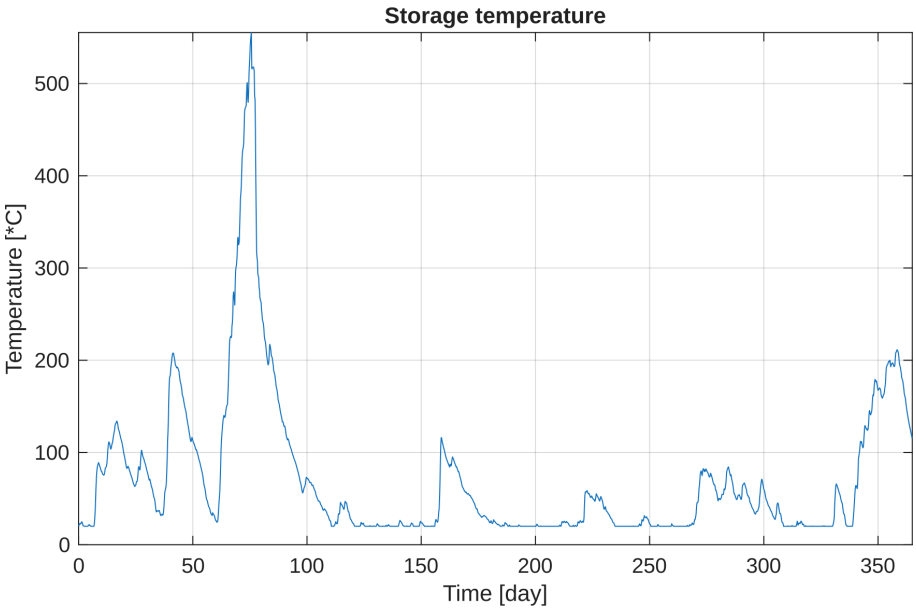

Figure 3: Storage temperature

The amount of water flowing through the system increases over time, which correlates with the energy released during system discharge periods. Figure 4 shows the total cumulative mass flow in the Rankine cycle of the extraction subsystem of the EST.

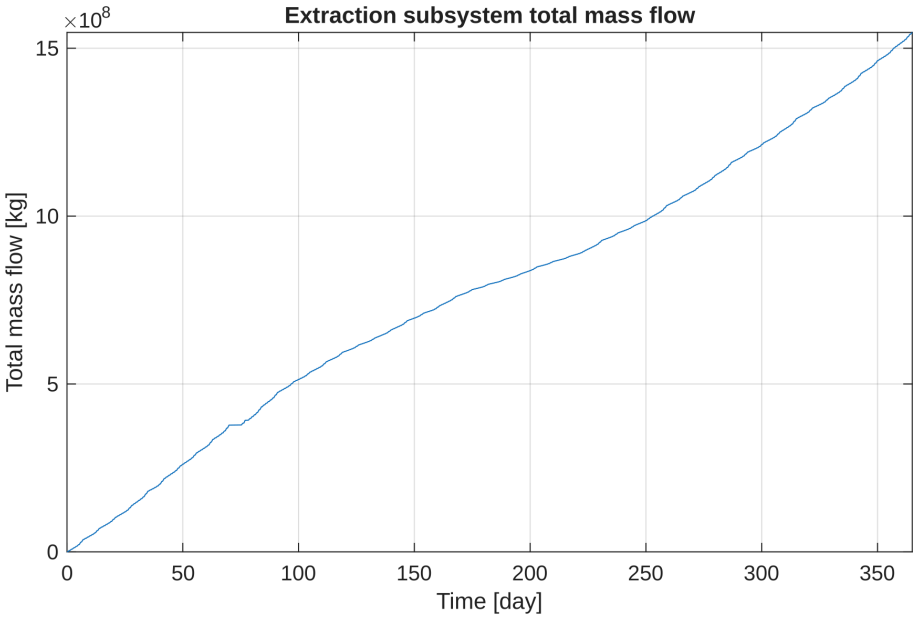

Figure 4: Extraction Subsystem Total Mass Flow

Looking at the total efficiency of the system, Figure 5 displays the divisions of how the supplied energy was stored and pushed to the demand. Currently, all the energy is stored that exceeds the demand, and only 21% of the requested electricity is bought.

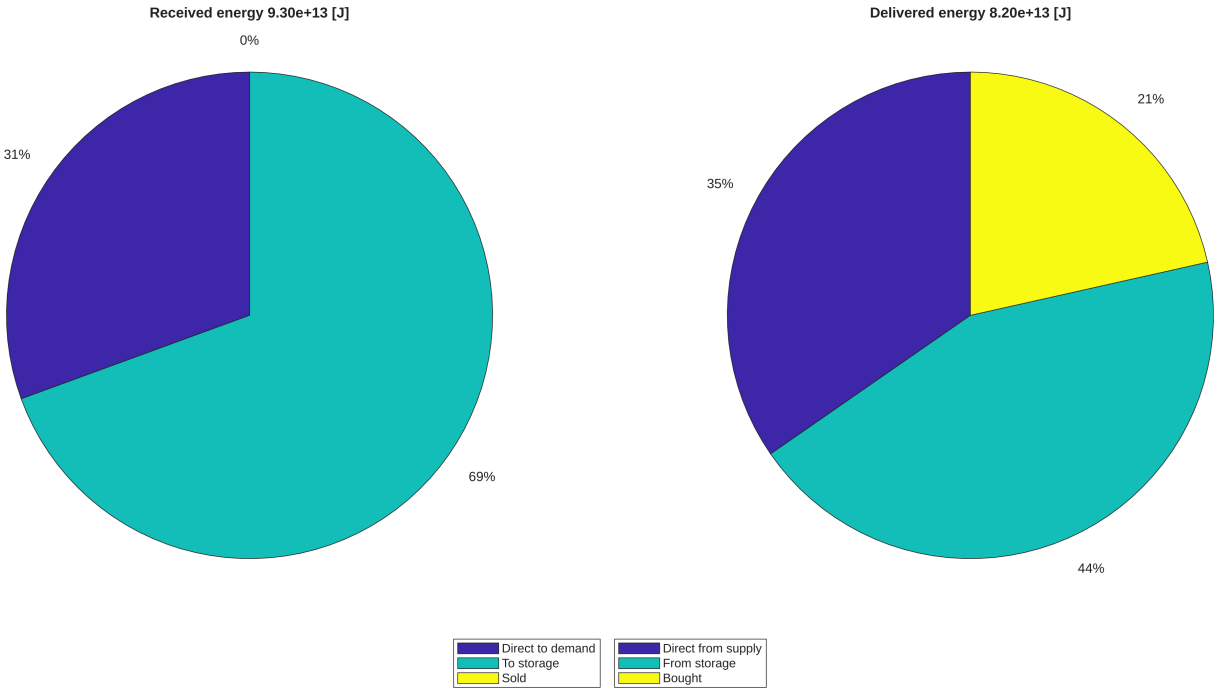

Figure 5: Energy usage

Having 44% of the total energy delivered from the battery shows its effectiveness. Without it, the amount of bought energy would effectively triple. This would increase costs for the residents and raise demand on the grid since this electricity would need to be supplied by other sources, which are potentially far from the location. Implementing the modeled battery would solve the design challenge while leaving room for future improvement, such as increasing the volume when the demand inevitably grows.

4 Model development reflection

4.1 The Simulink model

What physical parameters in the Simulink model can be varied to study their effect on the performance of the EST system? For each parameter, indicate the range for which you have tested your model.
Three key variables of the Simulink model were the geometry, the volume, and the pressures inside the Rankine cycle. Both cubic and cylindrical tanks were considered, and it was concluded that a cylindrical tank with a surface area of 3030 m^2 would lead to lower energy losses. By halving the volume, higher temperatures have been reached within the battery, increasing the Rankine cycle's efficiency, however, the overall efficiency was reduced by 15% due to the lower storage capacity. By changing the pressures within the Rankine cycle the output efficiency was shown to improve, however, the results were too small in magnitude.

What is the biggest limitation of the current Simulink model? What steps can be taken to improve the Simulink model w.r.t. this limitation?
The biggest limitation of the current Simulink model is its assumptions about an equal heat across the entire volume of the cylinder. In real life there would be a different heat in the bottom than in the top because the heated air will cool when reaching the top. In order to improve the Simulink model and include this behavior the following solution can be implemented. The cylindrical storage tank can be modeled as small slices, where the temperature is calculated within every slice individually. This way the temperature in the storage tank is more accurate, and then radiation between the rocks can be implemented in the model as well. This would result in the heating of the extraction-subsystem water in the storage tank modeled more realistically.

4.2 Relation with the validation experiment

Where in the Simulink model did you make use of the physical law studied in the validation experiment?
The physical law studied as part of the validation experiment was the conduction of heat within the solid block of the storage tank in Simulink. The experiment verified the medium- and long-term heat storage and heat dissipation capabilities within the storage medium itself, while accounting for convection losses. Later in the project, a modification was made to substitute the solid block of basalt with a porous medium, ensuring the model resembles the real-world scenario more closely. The validation experiment allowed cross-validation of assumptions made about the mechanisms and rate of energy loss within a theoretical, cylindrical-shaped heat storage tank.

To what extent do the conclusions regarding the validity of the studied physical law (as discussed in your Standard Operating Procedure) carry over to the real world EST system considered in your Simulink model? Think for example about the differences in time and length scales.
One of the main differences between the SOP and the proposed real-world model is the difference in the materials used in the heat storage tanks. The provided material in the experiment was aluminum which is different from the porous material chosen being basalt. This difference creates changes in energy. Another key difference is the time scale of both models. The validation experiment was not only executed at a lower temperature (60 °C instead of 600 °C), but also at a time scale reduced by several orders of magnitude (300 s instead of 300×10^5 s). These magnitude differences lead to differences between the model and the experiment. For example, at higher temperatures, radiation losses become more significant (proportional to T^4) and scaling time nonlinearly does not preserve the behavior of the losses.

4.3 Overall process

What is the most important lesson your group learned from the overall model development process, including both the Simulink model development and the validation experiment?
One of the key takeaways from the group project was the invaluability of good code documentation and clear commit messages. Using concise and descriptive git commit names allowed our group to improve the Simulink workflow, making it easier to track the evolution of different parts of the codebase and easily find rollback code when necessary. This has been further underscore by the binary nature of the Simulink/MATLAB files, making commit descriptions necessary to identify the content and/or changes made at a given stage to the virtual model. Another key takeaway from the group was the need for a comprehensive elaboration of how the written code works. The utilization of concise paragraphs in SSAs and clarifying comments inside the code block themselves make the model understanding a lot easier.

References

[1] H. Muller-Steinhagen, "RANKINE CYCLE," in *A-to-Z Guide to Thermodynamics, Heat and Mass Transfer, and Fluids Engineering*. Begellhouse, 2011.

[2] "STEAM TABLES," in *A-to-Z Guide to Thermodynamics, Heat and Mass Transfer, and Fluids Engineering*. Begellhouse, 2011.

[3] NASA, "GRCop-84: A High-Temperature Copper Alloy for High-Heat-Flux Applications," February 1, 2005, (Accessed 24/05/2025). [Online]. Available: https://ntrs.nasa.gov/citations/20050123582

[4] S. Soprani, F. Marongiu, L. Christensen, O. Alm, K. D. Petersen, T. Ulrich, and K. Engelbrecht, "Design and testing of a horizontal rock bed for high temperature thermal energy storage," *Applied Energy*, vol. 251, p. 113345, 2019. [Online]. Available: https://www.sciencedirect.com/science/article/pii/S0306261919310190

[5] C. Huang, Y. Wang, and W. Wang, "Design and optimization of a high-temperature rankine carnot battery," Sep. 2023. [Online]. Available: http://dx.doi.org/10.46855/energy-proceedings-10686

[6] Paul Wynns, "Pilot's Guide to Density of Air + Air Density Altitude Calculator," June 27, 2024, (Accessed 02/06/2025). [Online]. Available: https://aviex.goflexair.com/blog/density-of-air-air-density

[7] University of Sydney, "Formulas for Viscosity," 2005, (Accessed 02/06/2025). [Online]. Available: http://www-mdp.eng.cam.ac.uk/web/library/enginfo/aerothermal_dvd_only/aero/fprops/propsoffluids/node5.html

[8] Nuclear Power, "Supercritical Rankine Cycle," 2025, (Accessed 13/06/2025). [Online]. Available: https://www.nuclear-power.com/nuclear-engineering/thermodynamics/thermodynamic-cycles/rankine-cycle-steam-turbine-cycle/supercritical-rankine-cycle/

Attachments